ViPSN-Pluck: A Transient-Motion-Powered Motion Detector

Xin Li, *Graduate Student Member, IEEE*, Hong Tang, Guobiao Hu, Bao Zhao, *Graduate Student Member, IEEE*, and Junrui Liang, *Senior Member, IEEE*

***Abstract*—The emerging energy harvesting technology facilitates the development of ubiquitous and everlasting battery-free motion detectors. This article introduces a robust design of the transient-motion-powered motion detector, which is called ViPSN-pluck. "ViPSN" is the acronym for the vibration-powered sensing node while "pluck" stands for the plucking-motion energy harvester. By using a piezo-magneto-elastic structure, ViPSN-pluck can efficiently harvest energy from a transient motion. By properly making good use of this tiny harvested energy, ViPSN-pluck can effectively carry out motion detection and Bluetooth low-energy (BLE) wireless communication. Given the concurrency of mechanical potential energy precharging and motion detection, the transient-motion plucking energy harvester used in ViPSN-pluck has the merit of high energy reliability. This unique feature is unprecedented in the solar and radio-frequency (RF) energy harvesting cases, which might suffer from energy outages under fluctuating irradiance or RF signal strength, respectively. The working principle of ViPSN-pluck, in particular, the dynamic characteristics of the plucking energy harvester and the energy matching between generation and utilization, are discussed in detail to demonstrate the robustness in operation. The cyber-electromechanical synergy among the mechanical dynamics, power conditioning circuit, and low-power embedded system is highlighted. The design methodology of ViPSN-pluck provides a valuable reference for the developments of future motion-powered Internet of Things devices.**

***Index Terms*—Battery-free Internet of Things (IoT), energy harvesting, motion detector, plucking, ubiquitous sensing.**

I. Introduction

MOTION detection plays an essential role in security surveillance [1], intruder detection [2], occupancy identification [3], activity monitoring [4], smart building [5], [6], etc. Motion detectors should be economical and robust, such that they can be massively deployed and offer pervasive service to support various smart applications [7]. Existing motion detecting technologies are mostly based on visual [8], [9], infrared [10], mechanical [11], or audio [12] sensors. Some are expensive and require complex installation. Moreover, most of these motion detecting devices are still powered by grid power or chemical batteries. As the number of nodes increases, electrical wiring or battery maintenance costs considerable money and human effort. Therefore, battery-free and maintenance-free solutions are necessary for the ubiquitous and everlasting deployment of massive motion detectors.

Energy harvesting, as an emerging technology in the last two decades, aims to scavenge wasted energy from the ambiance. It provides promising solutions to address the sustainable power supply issue and facilitates the realization of battery-free and maintenance-free Internet of Things (IoT) devices. The battery-free motion-sensing devices powered by ambient solar photovoltaic (PV), radio-frequency (RF), or kinetic energy, have attracted numerous research interests in recent years. For instance, a series of RF-powered passive tags has been built for motion monitoring [13], [14]. Solar-powered smart on/off body sensing devices have been developed to record and infer human activities and interactions [15], [16]. The design of battery-free cameras has been extensively explored by considering the issues from various perspectives, including the harvesting sources [17], wireless communication [18], and system architectures [19], [20].

Like most of the renewable energy sources, the ambient energy sources are volatile, i.e., it often fluctuates with time. Therefore, energy-harvesting-powered IoT devices are remarkably different from their conventional battery-powered counterparts because the variable ambient power supply violates the basic assumption of battery-powered devices—a stable energy supply [21], [22]. The sensing, computing, and communicating tasks in battery-free systems need to be redesigned to better meet with the unstable power supply [23]. It is challenging that, even with some cutting-edge techniques, such as progress checkpointing [24], special debugging tools [25], and finely tuned or reconfigurable power supply strategies [26], energy-harvesting-powered devices are still less reliable than their battery-powered counterparts [27].

In PV, RF, and most kinetic energy harvester (KEH) cases, the harvested power is accumulated or buffered in the electrical domain after energy transduction. On the other hand, given its

Manuscript received February 25, 2021; revised June 9, 2021 and July 1, 2021; accepted July 12, 2021. Date of publication July 19, 2021; date of current version February 21, 2022. This work was supported in part by the Natural Science Foundation of Shanghai under Grant 21ZR1442300; in part by the ShanghaiTech University under Grant F-0203-13-003; and in part by the Shanghai Key Laboratory of Mechanics in Energy Engineering under Grant ORF-202001. *(Corresponding author: Junrui Liang.)*

Xin Li is with the School of Information Science and Technology, Shanghai Engineering Research Center of Energy Efficient and Custom AI IC, ShanghaiTech University, Shanghai 201210, China, also with the Shanghai Institute of Microsystem and Information Technology, Chinese Academy of Sciences, Shanghai 200050, China, and also with the University of Chinese Academy of Sciences, Beijing 100049, China (e-mail: lixin1@shanghaitech.edu.cn).

Hong Tang, Guobiao Hu, Bao Zhao, and Junrui Liang are with the School of Information Science and Technology, Shanghai Engineering Research Center of Energy Efficient and Custom AI IC, ShanghaiTech University, Shanghai 201210, China (e-mail: tanghong@shanghaitech.edu.cn; hugb@shanghaitech.edu.cn; zhaobao@shanghaitech.edu.cn; liangjr@shanghaitech.edu.cn).

Digital Object Identifier 10.1109/JIOT.2021.3098238

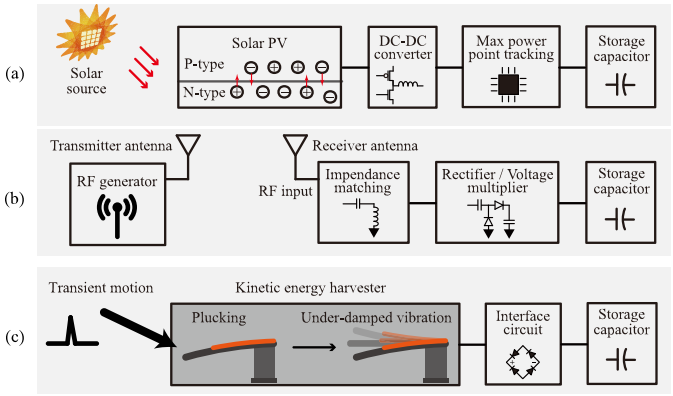

Fig. 1. Comparison of energy harvesting technologies. (a) Solar energy harvesting based on photovoltaic (PV) effect. (b) Radio-frequency (RF) energy harvesting through electromagnetic transmission. (c) Motion energy harvesting via a plucking mechanism. Energy reliability is guaranteed by properly designing the potential energy precharging process.

low-frequency operation and affluent dynamics, a KEH can be better designed to match the source feature by making some specific mechanical modulations [28]. For example, to harness energy associated with slow motion, frequency up-conversion designs, such as the plucking mechanism, are usually utilized. A plucking KEH buffers energy in the mechanical domain and later carries out electromechanical transduction, as illustrated in Fig. 1(c). The mechanical-to-mechanical energy conversion has a perfect coupling coefficient and rapid conversion speed if inertia is sufficiently small. Therefore, the motion energy can be more determinately extracted, in the form of potential energy, for reliably powering some IoT tasks within the lower bound of harvested energy. Such a feature of the buffer-then-convert KEH designs is unique, compared with the PV and RF cases, as well as their convert-then-buffer KEH counterparts [29]. Since the "energy packet" of every single plucking motion is deterministic, the reliability of IoT operations is reinforced.

The plucking mechanism was extensively studied to broaden the energy harvesting bandwidth, in particular, to improve the electromechanical conversion under low vibration frequency [30], [31]. However, nearly all literature about plucking KEH focused on only mechanical dynamics and continuous plucking motions, where harvested power rather than energy was emphasized; the electrical dynamics is simply taken as a linear resistor; no IoT element was included [32], [33]. On the other hand, in other studies focusing on the motion-powered IoT design, only the simplest linear mechanical harvester was used [34], [35]. The mechanical dynamic effect was even neglected for simplicity in some studies [36]. In a word, few studies have investigated or even discussed the synergy among all essential mechanical, electrical, and cyber parts toward a practical transient-motion-powered IoT application yet.

Given the aforementioned challenge and insufficiency in system-level studies, this article introduces a systematic design of a transient-motion-powered sensing node, which is called ViPSN-pluck in short. ViPSN-pluck has integrated energy harvesting, motion detection, and wireless communication functions. In particular, the plucking design enables concurrent motion energy harvesting and motion information acquisition. The harvested energy is sufficient to power some specific sensing, computing, and wireless communication functions. Instead of relying on continuous motions, such as walking and running, ViPSN-pluck explores an extreme excitation scenario by making use of a single plucking motion, which is discrete and instantaneous. The plucking KEH can be regarded as a mechanical modulator, where mechanical potential energy is precharged before mechanical-to-electrical energy transduction takes place. The potential energy precharging action guarantees the lower bound of harvested energy from a transient motion, such that the IoT tasks, including motion pattern identification and wireless communication, can be reliably executed.

There are three major highlights for this ViPSN-pluck design, which are listed as follows.

1) ViPSN-pluck presents a pioneering design toward robust transient-motion-powered IoT applications.
2) By emphasizing the potential energy precharging process, ViPSN-pluck raises the attention toward energy-oriented KEH-IoT designs.
3) By properly correlating the motion energy generation and motion direction detection and making a cyber-electromechanical co-design, ViPSN-pluck introduces a novel battery-free sensing architecture for motion detection.

II. Related Work

A. Motion Detection

The existing human motion detection is realized through either device-based or device-free solutions. Their features and principles are briefly reviewed and summarized as follows.

Device-Based: Conventional human motion detection requires the users to wear inertia measurement units (IMUs), including accelerometers and gyroscopes [37], [38]. The IMU can provide accurate measurements of motion data. However, the installation and frequent battery recharging are inconvenient and troublesome [39]. Recently, much effort has been devoted to developing battery-free wearable motion detectors. CapBand [15] was designed to recognize human hand gestures by sensing small skin movement of the human wrist via a successive capacitance measurement technique. The system is powered by a solar energy harvesting module. On the other hand, there are some designs powered by the RF energy harvesting technique. For example, a stretchable and flexible skin-interfaced sensing system introduced in [40] was used to record continuous and clinical vital physiological parameters. Its sweat sensor generates electrical signals that are proportional to the concentration of target analytes. It operates like a biofuel cell [41]. In addition, thermoelectric conversion has also been applied to produce electricity from body temperature gradient for powering wearable devices, such as a wristwatch [42], a forehead headphone [43], and other medical sensors [44], [45].

Device-Free: To get rid of the wearable burden, noncontact sensors, including cameras [46], passive infrared sensors,[10],

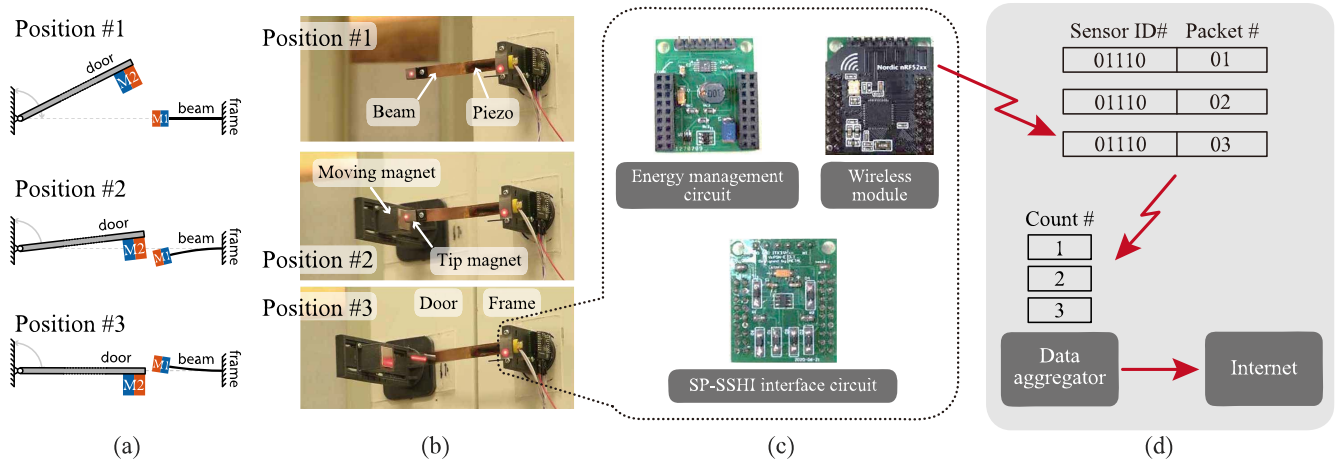

Fig. 2. ViPSN-pluck architecture. (a) Top view of the plucking KEH in three positions. (b) Field installation. (c) ViPSN modules. (d) Data aggregator.

audio-based sonar systems [12], or RF identification platforms [7], [47] were used for building device-free motion detection system. However, these systems have some drawbacks, such as limited information and restricted sensing area, due to ambient noise, weak echo signals, multipath effects, etc. Moreover, the maintenance of a large number of ubiquitous sensors for supporting an everlasting operation is extremely troublesome.

The maintenance problem might be solved by introducing energy harvesting-based battery-free solutions. For example, WISPCam [18], [19], which is remotely powered by an RFID reader, could realize reliable image capture for motion recording and surveillance. The passive RFID tag itself can also be used for motion detection and human tracking. An intrusion detection system, named Twins, was developed based on this principle by leveraging the interference among two passive tags for movement detection [1]. OptoSense [16] is a self-powered sensing system that can infer user activities and interactions according to ambient light intensity. In OptoSense, the ambient light not only generates sensing signals but also supplies energy to support the IoT operations.

B. Kinetic Energy Harvesting

Energy harvesting from human or machine motions is one of the most promising sustainable energy solutions for massively deployed IoT devices [48]. The daily energy consumption of a normal human being is about 1.07×10^7 J, which indicates that the average power is 124 W [49]. Most of the energy is wasted in body motions [50]. Different efforts have been made to extract energy from human motions, such as joint rotation, foot strike, or limb swing and convert the extracted energy into useful electricity [51]. However, human motions are generally in the low-frequency range, i.e., about 0.2–10 Hz. On the other hand, electromechanical transducers generate more power around their resonant frequencies, whose range is around 60–180 Hz. Therefore, to match the preferred frequency ranges of the source and energy harvester, mechanical modulation designs are often needed [28]. The extensively studied mechanical modulation methods for harnessing energy associated with the low-frequency movement are referred to as the frequency up-conversion mechanisms.

Frequency Up-Conversion: Given the large potential demand for self-powered wearable electronics, various frequency upconversion designs have attracted much research interest in recent years [52]. According to the literature, the existing frequency upconversion methods can be summarized and classified into three major categories: 1) impact-based; 2) snap-through; and 3) plucking designs. Among these solutions, the plucking approach has been used to design many energy harvesters that harness different human motions, such as limb movement [53], [54] and knee-joint rotation [55]–[57]. As illustrated in Fig. 1(c), a plucking motion refers to an action that pushes/pulls a harvester structure away from its elastic equilibrium and then quickly releases it after a certain critical point. The critical releasing point defines the precharged energy in the form of mechanical potential energy. After release, the structure starts an underdamped vibration at its resonant frequency, which is usually higher than that of the driving motion. In this way, the KEH always transiently operates around its resonance, where the transduction power is maximized. The previous studies of plucking KEH focused on the power generation after the frequency upconversion from a low-frequency vibration to high-frequency transient underdamped vibrations without considering any end applications [32], [58]–[60].

When being fully linked with the information demand, it turns out that only a single plucking motion can reliably fulfill fundamental IoT detection and connection. Since we only consider the application of a single plucking motion, the harvested energy, rather than power, is regarded as the key factor for evaluating the feasibility of the plucking KEH in this study.

III. System Overview

The system architecture of ViPSN-pluck, including its mechanical structure for energy harvesting and motion sensing, circuit modules, and data transmission scheme, is illustrated in Fig. 2.

The main structure is a piezoelectric cantilevered beam, which is fixed at the door frame, and a pair of repelling magnets, which are installed at the beam's free end (M1) and the moving door (M2), respectively, as shown in Fig. 2(a) and (b). The three representative positions during the open-door and close-door motions are denoted as positions #1–#3, respectively. In the close-door motion, the door magnet moves through position #1 to position #2 successively and stops at position #3; while in the open-door motion, the door magnet starts from position #3 and moves through position #2 and #1, successively. In either the open-door or close-door motions, the door magnet induces a magnetic plucking action to the piezoelectric cantilever, such that to trigger its transient underdamped vibrations. Energy is harvested in the meanwhile of underdamped vibration.

In order to tell the open-door and close-door motions, the two plucking motions are intentionally designed to be asymmetric by introducing a horizontal misalignment between the center of door magnet M2 and the equilibrium position of beam magnet M1 when the door is closed. Therefore, the amounts of accumulated energy after the two motions are different. Since the harvested energy is approximately proportional to the transmitted packets, the direction information can be obtained by the receiver by simply counting the packet number. The working principle and dynamics of the plucking KEH are discussed in detail in Section IV.

After the plucking KEH, the harvested energy is conditioned in the electrical domain. The development platform ViPSN has provided a well-rounded solution for energy enhancement, energy management, and fundamental IoT applications [61]. The three ViPSN modules used in this design are shown in Fig. 2(c). A self-powered synchronized switch harvesting on inductor (SP-SSHI) power-boosting interface circuit is used in ViPSN-pluck for enhancing the energy harvesting capability [62]. The energy management circuit carries out voltage regulation with the awareness of the energy storage level. The wireless module sends out Bluetooth low-energy (BLE) signals whenever a sufficient amount of energy is collected.

The data aggregator, whose scheme is illustrated in Fig. 2(d), listens for packets from one or multiple ViPSN-pluck motion detectors. Upon packet reception, it counts the number of received packets to identify the motion direction accordingly. Moreover, the data aggregator could also archive the data for historical analysis or send them to the cloud for further analysis, processing, and visualization. In this design, the standard BLE beacon protocol is utilized to broadcast the motion detection information. Thus, any Bluetooth device, such as a smartphone and laptop computer, can work as a data aggregator.

IV. Plucking KEH Principle

The transient plucking KEH plays an essential role in guaranteeing the performance of ViPSN-pluck. From the energy supply point of view, the transient-motion harvester should harvest sufficient energy during a single plucking motion for supporting the operation of ViPSN-pluck. To enhance the robustness of sensing, computing, and communication and the success rate of direction identification, the mechanical structure must be carefully designed.

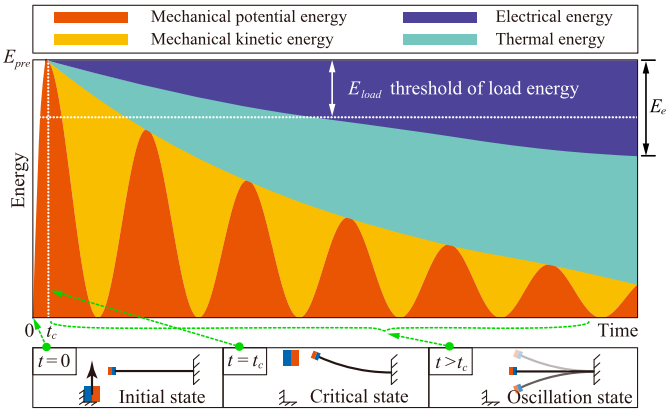

Fig. 3. Energy flow dynamics of an energy harvester under a plucking excitation.

A. Transient-Motion Harvester

One of the transient-motion-powered motion detectors is installed at the front door of our laboratory. A piezoelectric cantilevered beam with a tip magnet M1 is installed at the stationary door frame, while the driving magnet M2 is installed at the moving door. During the transient open-door or close-door movements, the driving magnet M2 skims the vicinity of the tip magnet M1. The magnetic force pushes M1 away from its equilibrium. After the tip magnet M1 is brought to a critical position, where the magnetic force could not balance the restoring force of the bending beam, the piezoelectric cantilevered beam is rapidly released. After being released, the cantilevered beam starts to oscillate until the vibration is damped out. In general, a plucking action can be divided into two phases before and after the critical point, i.e., mechanical potential energy precharging and decaying underdamped-free vibration. Instead of expecting a continuous power supply from the harvester, we are interested in how much energy can be harvested from a transient motion, because the harvested energy in a transient determines the run-time behavior of ViPSN-pluck, such as when to execute tasks, when to switch to low-power mode, and when to start communication.

B. Potential Energy Precharging

Fig. 3 shows the energy flow dynamics under a single plucking excitation. There are four forms of energy involved in this process: 1) mechanical potential energy; 2) mechanical kinetic energy; 3) thermal energy; and 4) electrical potential energy. The energy transformations during this process can be summarized as follows.

1) Plucking Start: At the beginning, the energy harvester is at its equilibrium position. We set this position the zero-energy position.

2) Energy Accumulation: As the driving magnet forces the cantilevered beam to deform, it does positive work to the cantilevered beam. Assuming a very slow plucking motion, in which the kinetic energy can be neglected, the input energy

is collected by the deformed cantilevered beam in the form of strain energy, i.e., the mechanical potential energy of a deformed structure. The potential energy reaches its maximum when the cantilevered beam arrives at the critical position. The total mechanical potential energy at M1 position w and M2 position b can expressed as follows:

$$U(w, b) = \frac{1}{2}Kw^2 + \int F_m \cos\theta \, \mathrm{d}(b - w) \tag{1}$$

where K is the equivalent stiffness of the beam; w is its tip deflection; b is the position of the driving magnet M2, F_m is the magnetic force, θ is the angle between the repelling magnetic force F_m and movement direction w. The beam deforms until it arrives at the critical position b_c (the very instant is denoted as t_c), where the magnetic force is no longer sufficiently large to counteract the elastic force. At this critical position, the potential energy stored in the cantilevered beam reaches a maximum, as shown by the t_c instant in Fig. 3. The work done by the moving magnet is converted into the potential energy, which is stored in the deformed beam. Therefore, this process is called *potential energy precharging*. The precharged potential energy is a function of the two displacements of M1 and M2 at the critical instant, i.e.,

$$E_{\text{pre}} = U[w_c = w(t_c), b_c = b(t_c)]. \tag{2}$$

3) Underdamped Vibration: After passing through the critical point, the cantilevered beam is released from the magnetic lock. It tends to return to its equilibrium position. Since the beam is an underdamped vibrator, it starts a decaying vibration around its equilibrium position under its resonant frequency, as shown in Fig. 3. During the free vibration, the precharged potential energy (E_{pre}) (illustrated in red) is first converted into the mechanical kinetic energy (in orange), then back into potential energy, and back and forth repeatedly. In the meantime, due to the presence of mechanical damping, a part of the energy is dissipated, i.e., converted into thermal energy (in cyan). On the other hand, because of the piezoelectric transducer, a part of the energy is converted into electrical energy and stored in the electrical storage devices, a small capacitor in this study. Since the driving magnet only does work in the precharging phase, the precharged potential energy E_{pre} determines the level of total energy income in a single plucking motion.

In practice, given that the door speed is larger than the quasistatic case, the input energy is actually larger than that in the aforementioned slow motion case. In particular, with the increase of the door speed, the initial kinetic energy increases. Hence, the lower bound of precharged energy is guaranteed. Later experiment shows that, at normal door speeds, the initial kinetic energy is usually much smaller than the initial potential energy. The lower bound of precharged energy can be adjusted by tuning the mechanical structure features, such as the beam geometries (related to elastic potential) and the horizontal gap between magnets M1 and M2 (related to magnetic potential).

A parameter η is introduced to denote the electromechanical energy conversion efficiency, which is related to the mechanical structure, interface circuit, and energy management unit. The harvested electrical energy, therefore, can be simply taken as part of the precharged energy $E_e = \eta E_{\text{pre}}$. Only when the harvested energy E_e exceeds the kicking-off threshold of ViPSN-pluck, which is denoted as E_{load}, the sensing and wireless communication functions can be fulfilled successfully. Given that the energy consumption of some specific software operations, such as initialization, sensing, and transmitting, is normally fixed, the energy reliability of ViPSN-pluck can be reinforced by carefully measuring the energy demand of the specific IoT functions, designing the mechanical structure, and further making sure $\eta E_{\text{pre}} > E_{\text{load}}$. Such a prechargeable feature before energy transduction is unique in mechanical or motion energy harvesters, compared to their PV and RF counterparts.

C. Potential Energy Pictures

The working principle of the plucking energy harvester and its motion detection function can be better elaborated by looking into its potential energy pictures. Figs. 4 and 5 show the varying potential wells in either open-door or close-door motions, respectively. The potential energy profile progressively changes along with the driving magnet movement. Each plucking motion drives the single-well monostable system to a bistable system, then to another monostable system. Yet, the starting and stopping potential wells are different.

The pictures of the open-door case are shown in Fig. 4. In the beginning, as shown in Fig. 4(a), the cantilevered beam stays still. Due to the presence of the driving magnet M2, whose resting position has a small offset to the right of the beam equilibrium, the cantilevered beam is slightly bent to the left-hand side. From the potential energy profile shown in Fig. 4(f), the magneto-elastic system is a monostable system since there is only one potential well-1. When the driving magnet moves to the left, the cantilever is further bent. A second shallower potential well-2 emerges, as shown in Fig. 4(g). The magneto-elastic system transits from a monostable system to a bistable one. In the following phases, the potential profile evolves from asymmetric [see Fig. 4(g)] to symmetric [see Fig. 4(h)], then to another asymmetric [see Fig. 4(i)] states. Finally, when the driving magnet moves far away from the cantilever harvester, the effect of the driving magnet is negligible. Therefore, the potential profile becomes a linearly symmetric case. The cantilevered beam undergoes a linear underdamped vibration, as shown in Fig. 4(j).

For the close-door case, the evolving pictures are illustrated in Fig. 5. Compared to the open-door case shown in Fig. 4, the process of the close-door motion is reversed. It starts from a linear state and ends at a nonlinear monostable state. The potential pictures from Fig. 4(g)–(i) and Fig. 5(g)–(i) are symmetric. The only difference to distinguish the plucking directions is from the depths of their corresponding final potential wells. The deeper the final potential well, the more energy is generated. As the moving magnet stops at negative infinity in the open-door case and the rest position b_t in the close-door case, respectively, an asymmetrical design is realized. Since the final well of the transient-motion harvester in the close-door process is shallower, the harvested energy in the close-door process is less. According to this feature, the

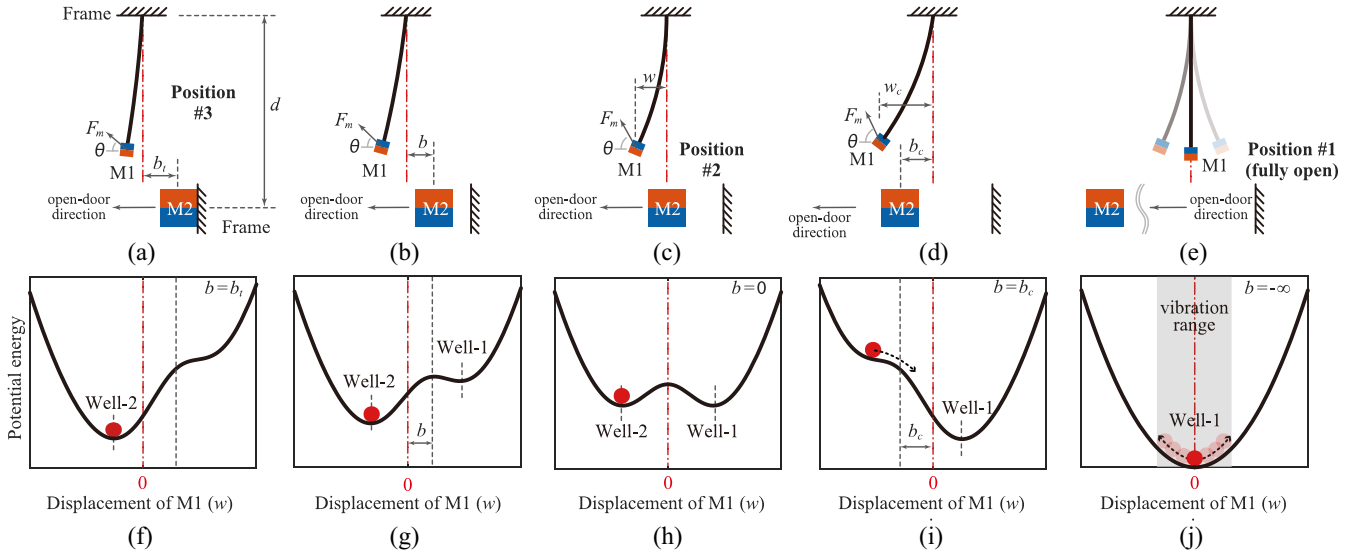

Fig. 4. Plucking dynamics in the open-door movement. (a)–(e) Beam positions. (f)–(j) Potential energy pictures. (a) and (f) Starting position #1 with a monostable potential well. (b) and (g) Intermediate position with two asymmetric wells. (c) and (h) Intermediate position #2 with two symmetric wells. (d) and (i) Critical position at which the energy barrier disappears. (e) and (j) Final position #3 ending up with the beam vibration in a single linear well.

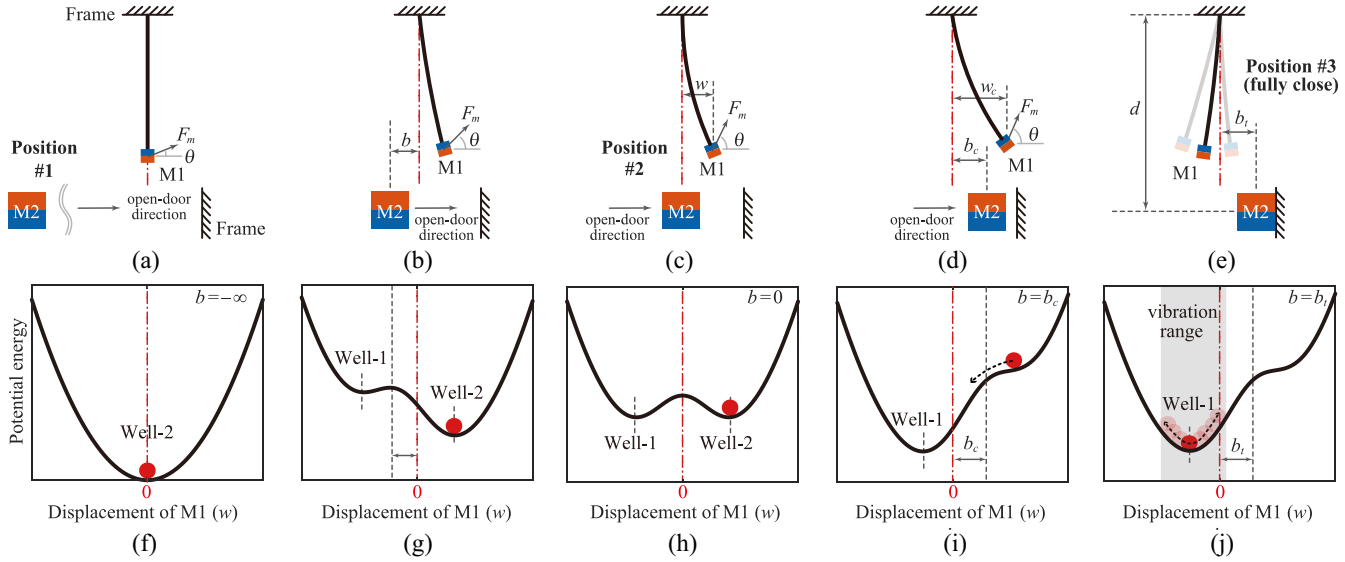

Fig. 5. Plucking dynamics in the close-door movement. (a)-(e) Beam positions. (f)-(j) Potential energy pictures. (a) and (f) Starting position #3 with a single linear potential well. (b) and (g) Intermediate position with two asymmetric wells. (c) and (h) Intermediate position #2 with two symmetric wells. (d) and (i) Critical position at which the energy barrier disappears. (e) and (j) Final position #1 ending up with the beam vibration in a monostable nonlinear well.

motion direction can be differentiated based on how much energy is captured during a single plucking excitation.

The potential energy picture of any bistable or monostable system can be described with a third-order polynomial as follows [63], [64]:

$$U(w) = \frac{1}{2}(K-\alpha)w^2 + \frac{1}{3}\beta w^3 + \frac{1}{4}\gamma w^4 \tag{3}$$

where α, β, and γ are the polynomial coefficients to approximate the magnetic potential. They represent the additional linear, quadratic nonlinear, and cubic nonlinear stiffnesses, respectively, which are brought in by the magnet pair. Once the magnetic strengths of the magnets are provided, these three parameters are related to the distance b, the position of the driving magnet M2.

As shown in Fig. 4(c) and (h) and Fig. 5(c) and (h), when the driving magnet M2 arrives at position #2, we have $\beta = 0$. At this position, we obtain a symmetric double-well bistable potential profile. As the driving magnet slightly moves away from position #2 to either direction, β becomes positive (close-door) or negative (open-door). The two potential wells become asymmetric. The potential barrier is separating the two wells decreases as β getting more positive or negative. For example, in the open-door motion, as the left well-1 gets elevated and the right well-2 gets deepened gradually, the left well-1 will eventually disappear, as shown in Fig. 4(i). After passing through the critical position, only the

TABLE I
VIPSN-PLUCK SPECIFICATIONS

Module	Specification		
Energy harvester	Transducer	Size	8×50 mm^2
		Material	PZT
	Beam	Size	$100\times10\times0.53$ mm^3
		Material	Copper sheet
	Magnet	M1	$10\times10\times10$ mm^3
		M2	$20\times20\times20$ mm^3
	Deployment Configuration	d	150 mm
		b_t	30 mm
Interface circuit	Parallel-SP-SSHI [65]		
Energy management circuit	DC-DC	LTC3588-1 [66]	
	Comparator	MIC841 [67]	
	Storage	10 μF capacitor	
Wireless module	Hardware	nRF52832 [68]	
	Software	BLE beacon	

TABLE II
ENERGY STATISTICS

Operation	Energy (μJ)	Duration (ms)
micro-controller initialization	72.70	53.8
Radio initialization	68.47	13
Beacon broadcasting	60.37	5

right well-2 lefts. The cantilevered beam is trapped in well-2 and vibrates, as shown in Fig. 4(j). The mathematical model helps describe the evolution of potential wells in either motion direction.

V. IMPLEMENTATION AND EVALUATION

A. Hardware Platform

The prototype of ViPSN-pluck is shown in Figs. 2 and 8. A piezoelectric cantilever is used as the kinetic transducer. The holding fixture of the transient-motion energy harvester is manufactured using a 3-D printer. The other three circuit units are developed based on ViPSN [61], an opensource development platform for vibration-powered IoT devices.[1] The specifications of ViPSN-pluck are listed in Table I. In the energy management circuit, an LTC3588-1 IC [66] developed by Linear Technology Inc. is adopted for voltage regulation. It integrates a low-loss full-wave bridge rectifier and a high-efficiency buck converter. MIC841 [67], a micropower precision-voltage comparator with adjustable hysteresis, is used to detect the energy level of the storage capacitor. A 10-μF storage capacitor, which satisfies the minimum energy demand for at least two rounds of IoT operations, is selected. A programmable nRF52832 BLE system on chip (SoC) by Nordic Inc. [68] is utilized for sensing and wireless communication. A smartphone is used as a data aggregator. It receives the packets from ViPSN-pluck, processes the data, and handles the Internet connection.

B. Basic Operation

Fig. 6 shows the energy, supply, and load current in a complete operation cycle of ViPSN-pluck when it is activated. After a single plucking excitation, as some potential energy is converted into electricity via the beam energy harvester,

[1]https://github.com/METAL-ShanghaiTech/ViPSN

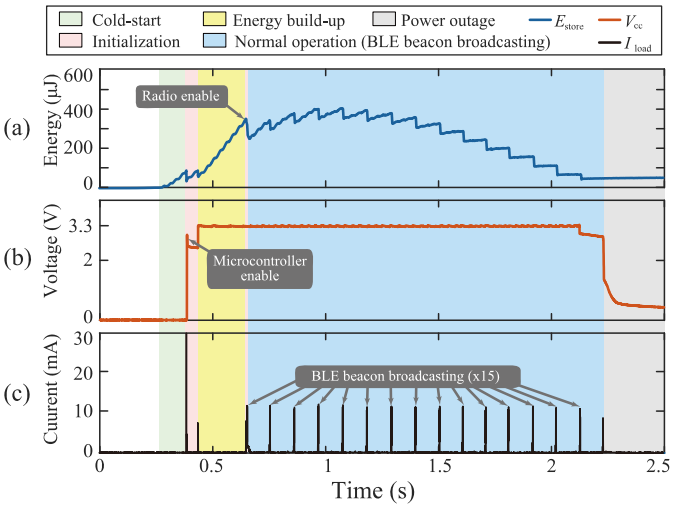

Fig. 6. Workflow of ViPSN-pluck during one plucking motion. (a) Storage energy E_{store}. (b) DC voltage output V_{cc}. (c) Load current.

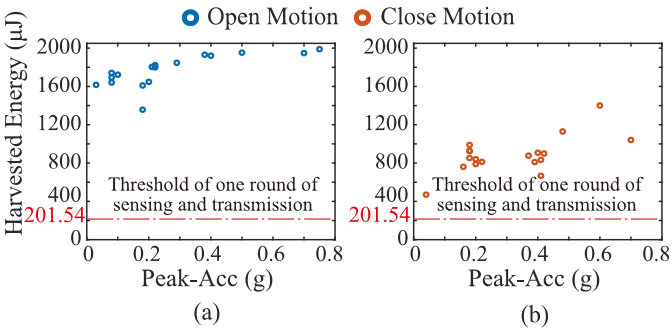

Fig. 7. Measured harvested energy under different door speeds. (a) Open-door motion. (b) Close-door motion.

the storage energy E_{store} increases. When it reaches a specific threshold, the buck converter in LTC3588-1 is activated to provide a regulated 3.3-V voltage supply to boot up the microcontroller, as shown by the steep rising edge in Fig. 6(b). Subsequently, after a brief energy rebuild-up phase (in yellow), robust radio wake-up is robustly achieved without meeting unexpected energy outages. As a result, BLE beacon packets can be sent out later at a constant time interval. As shown in Fig. 6(c), more than 15 BLE beacon packets are sent out after one plucking motion. The number of the BLE beacon packets also implies information about the harvested energy level from this specific plucking action. Finally, at the end of this operation cycle, the microcontroller exits the active mode, and the LTC3588-1 disconnects the voltage supplier. The system enters the deep-sleep mode and waits for the next plucking excitation.

C. Energy Reliability

Fig. 7 shows the energy harvesting performance of the ViPSN-pluck prototype under open-door and close-door excitations. Experiments are carried out under different door accelerations, whose peak values range from 0.03 to 0.6 g. Experimental results demonstrate that during either the open-door or close-door process, ViPSN-pluck can robustly harvest

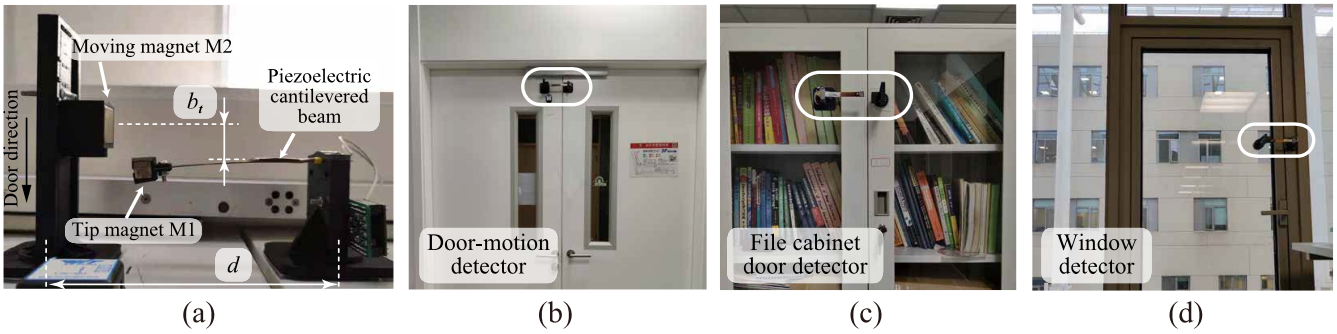

Fig. 8. ViPSN-pluck prototypes in field tests. (a) Deployment configuration. (b) Door motion detector. (c) File cabinet door detector. (d) Window detector.

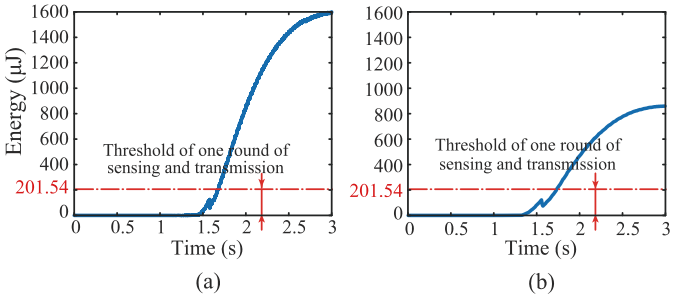

Fig. 9. Charging history. (a) Open-door motion. (b) Close-door motion.

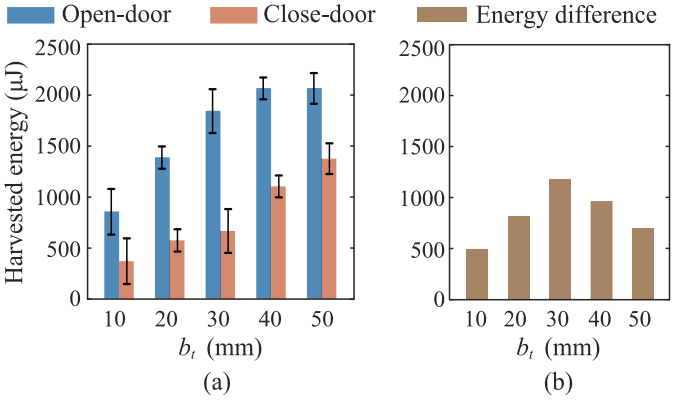

Fig. 10. Harvested energy under different b_t, the rest position of M2. (a) Harvested energy with different motions. (b) Difference in average energy.

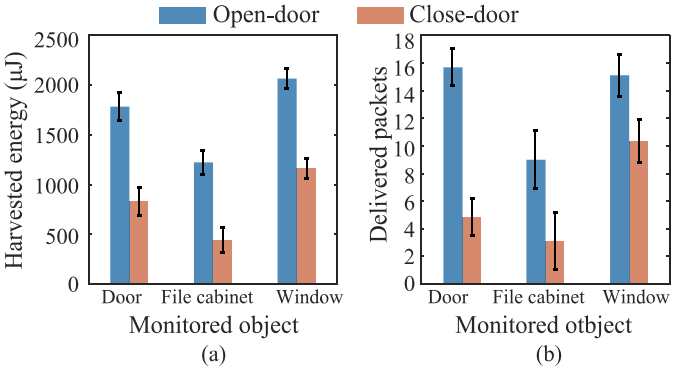

Fig. 11. Performance of ViPSN-pluck in several real-world scenarios. (a) Harvested energy from several object movements. (b) Delivered packets.

at least 400-μJ electrical energy. Given the nominal energy consumption of a BLE IoT operation, including the three functions listed in Table II, is about 201.54 μJ, the harvested energy from a single open-door or close-door motion can satisfy the energy demand of ViPSN-pluck.

D. Motion Direction Identification

From the experimental results shown in Fig. 9(a) and (b), we can see that, for this ViPSN-pluck prototype, the harvested energy can be accumulated to about 1600 and 850 μJ in open-door and close-door motions, respectively, in around 1 s. Fig. 10(a) shows the measured harvested energy under different rest positions of the driving magnet M2, i.e., b_t parameter. Fig. 10(b) shows the average energy differences under different b_t. As mentioned in Section IV-C, the dynamic behavior of the asymmetric well can be set by tuning b_t. When b_t is larger, the magnetic force produced by M2 and applied to the tip magnet M1 becomes weaker. Therefore, the depth of the final asymmetric well-1 is closer to that of the linear well-2. The harvested energy in the two plucking directions are closer under large b_t. On the other hand, for the plucking motion in either direction, if b_t is too small, i.e., the M2 rest position is closer to the M1 equilibrium, the initial well is too shallow to provide large input energy. It can be observed from the measurement results shown in Fig. 10(a) that less energy is harvested under smaller b_t. Therefore, the energy difference between open-door and close-door processes can be optimized by tuning the rest position of the driving magnet M2. The different harvested energy under different b_t is shown Fig. 10(b). We set b_t to 30 mm in all experiments since it gives the most significant energy difference for better plucking direction identification.

The software code of ViPSN-pluck is optimized to ensure a rapid and robust response. Each plucking activation consists of one initialization and several radio transmissions. The energy consumption for each operation is rather stable as listed in Table II. Since the energy consumption of a beacon broadcasting is almost the same, about 60.37 μJ, the harvested energy is roughly proportional to the possible sent-out packets. By counting the number of BLE beacon packets received by the data aggregator, as illustrated in Fig. 2(d), the plucking direction can be identified.

E. Field Test

After the experimental test to investigate the performance of ViPSN-pluck under various parameters, a field test is carried out to test the actual feasibility of ViPSN-pluck in real scenarios. Fig. 8 shows the field setup and the ViPSN-pluck prototypes installed in three field applications to detect and identify the open-door/close-door actions. The prototypes are installed at the front door, a file cabinet, and a window in our laboratory, as shown in Fig. 8(b)–(d), respectively. Table I and Fig. 8(a) show the specifications and deployment configuration.

Fig. 11(a) shows the harvested energy in the open-door/close-door motions in different scenarios. Fig. 11 shows the number of the delivered BLE beacon packets, which is recorded and counted by the data aggregator. In this field test, we use a smartphone as the system terminal. In different scenarios, there are some differences due to the influence of environmental conditions. For example, the material of monitored objects would affect the magnetic field of the magnets. As shown in Fig. 11(a), under the same configuration, the energy harvested by ViPSN-pluck deployed in the file cabinet (made of steel) is less than that in the window case (made of aluminum alloy) and that in the front doorcase (made of wood). In addition, there are also some differences due to the plucking kinetic energy fluctuates. But, in general, the experimental results show that the harvested energy is always more than the energy demand for a round of sensing and wireless transmission. At least 500 μJ of electric energy can be harvested to run the IoT functions. At least four beacon packets can be received to identify the motion directions.

Besides those scenarios shown in Fig. 8, ViPSN-pluck, as a self-powered motion detector, can also be deployed in many other applications, such as archives management, furniture safety, warehouse, and logistics. These realizations allow ViPSN-pluck to interconnect many moving things in the real world, either directly or indirectly.

VI. Conclusion

This article has presented a transient-motion-powered IoT motion detector, which is called ViPSN-pluck. It is developed based on a cyber-electromechanical synergetic co-design. The development of ViPSN-pluck involves knowledge from multiple disciplines, including mechanical dynamics, electrical power management, and low-power embedded systems. Through the sophisticated collaboration between the mechanical harvester configuration and software codes, the associated motion information can be sent out with an off-the-shelf BLE wireless module.

To address the sustainable power supply issue, a transient-motion harvester has been designed for ViPSN-pluck. Different from the solar or RF energy harvesting solutions, which might be constrained by fluctuating sources, the transient-motion harvester has a unique feature to provide a highly reliable energy supply to self-powered applications. Such a feature benefits from its potential energy precharging mechanism. To realize simultaneous motion detection, a novel motion detection mechanism has been conceived according to the dynamic characteristics of the transient-motion harvester. By making an asymmetric design, the amounts of harvested energy by the transient-motion harvester from different plucking directions are different. Owing to this feature, motion direction can be identified by counting the sent-out beacon packets, which are roughly proportional to the harvested energy. Therefore, in ViPSN-pluck, the energy harvester itself also acts another important part as the motion detector.

An experimental test has shown that the energy harvested from a single plucking excitation can be up to 2000 μJ, which is far more sufficient to power the basic operation of ViPSN-pluck. A field test in three real-world scenarios has validated the robustness of ViPSN-pluck for motion detection. In general, the work presented in this study provides valuable guidance for the design and development of future motion-powered IoT systems.

References

[1] J. Han *et al.*, "Twins: Device-free object tracking using passive tags," *IEEE/ACM Trans. Netw.*, vol. 24, no. 3, pp. 1605–1617, Jun. 2016.

[2] Z. Hussain, Q. Z. Sheng, and W. E. Zhang, "A review and categorization of techniques on device-free human activity recognition," *J. Netw. Comput. Appl.*, vol. 167, Oct. 2020, Art. no. 102738.

[3] S. Pan *et al.*, "FootPrintID: Indoor pedestrian identification through ambient structural vibration sensing," *Proc. ACM Interact. Mobile Wearable Ubiquitous Technol.*, vol. 1, no. 3, pp. 1–31, 2017.

[4] P. Zhang, S. Pan, M. Mirshekari, J. Fagert, and H. Y. Noh, "Structures as sensors: Indirect sensing for inferring users and environments," *Computer*, vol. 52, no. 10, pp. 84–88, 2019.

[5] J. Han, S. Pan, M. K. Sinha, H. Y. Noh, P. Zhang, and P. Tague, "Sensetribute: Smart home occupant identification via fusion across on-object sensing devices," in *Proc. 4th ACM Int. Conf. Syst. Energy Efficient Built Environ.*, 2017, pp. 1–10.

[6] S. Pan, M. Mirshekari, J. Fagert, C. Ruiz, H. Y. Noh, and P. Zhang, "Area occupancy counting through sparse structural vibration sensing," *IEEE Pervasive Comput.*, vol. 18, no. 1, pp. 28–37, Jan.–Mar. 2019.

[7] F. Zhang, C. Wu, B. Wang, H.-Q. Lai, Y. Han, and K. R. Liu, "WIDetect: Robust motion detection with a statistical electromagnetic model," *Proc. ACM Interact. Mobile Wearable Ubiquitous Technol.*, vol. 3, no. 3, pp. 1–24, 2019.

[8] L. Ren, A. Patrick, A. A. Efros, J. K. Hodgins, and J. M. Rehg, "A data-driven approach to quantifying natural human motion," *ACM Trans. Graph.*, vol. 24, no. 3, pp. 1090–1097, 2005.

[9] F. H. K. Zaman, H. Ali, A. A. Shafie, and Z. I. Rizman, "Efficient human motion detection with adaptive background for vision-based security system," *Int. J. Adv. Sci. Eng. Inf.*, vol. 7, no. 3, pp. 1–6, 2017.

[10] J. Yun and M.-H. Song, "Detecting direction of movement using pyroelectric infrared sensors," *IEEE Sensors J.*, vol. 14, no. 5, pp. 1482–1489, May 2014.

[11] S. Pan, M. Berges, J. Rodakowski, P. Zhang, and H. Y. Noh, "Fine-grained recognition of activities of daily living through structural vibration and electrical sensing," in *Proc. 6th ACM Int. Conf. Syst. Energy Efficient Build. Cities Transp.*, 2019, pp. 149–158.

[12] W. Ruan, Q. Z. Sheng, L. Yang, T. Gu, P. Xu, and L. Shangguan, "AudioGest: Enabling fine-grained hand gesture detection by decoding echo signal," in *Proc. ACM Int. Joint Conf. Pervasive Ubiquitous Comput.*, 2016, pp. 474–485.

[13] Y. Zhao, J. R. Smith, and A. Sample, "NFC-WISP: A sensing and computationally enhanced near-field RFID platform," in *Proc. IEEE Int. Conf. RFID (RFID)*, 2015, pp. 174–181.

[14] F. Zhang *et al.*, "Towards a diffraction-based sensing approach on human activity recognition," *Proc. ACM Interact. Mobile Wearable Ubiquitous Technol.*, vol. 3, no. 1, pp. 1–25, 2019.

[15] H. Truong *et al.*, "CapBand: Battery-free successive capacitance sensing wristband for hand gesture recognition," in *Proc. 16th ACM Conf. Embedded Netw. Sensor Syst.*, 2018, pp. 54–67.

[16] D. Zhang *et al.*, "OptoSense: Towards ubiquitous self-powered ambient light sensing surfaces," *Proc. ACM Interact. Mobile Wearable Ubiquitous Technol.*, vol. 4, no. 3, pp. 1–27, 2020.

[17] A. Saffari, M. Hessar, S. Naderiparizi, and J. R. Smith, "Battery-free wireless video streaming camera system," in *Proc. IEEE Int. Conf. RFID (RFID)*, 2019, pp. 1–8.

[18] S. Naderiparizi, M. Hessar, V. Talla, S. Gollakota, and J. R. Smith, "Towards battery-free HD video streaming," in *Proc. 15th USENIX Symp. Netw. Syst. Design Implement. (NSDI)*, 2018, pp. 233–247.

[19] S. Naderiparizi, A. N. Parks, Z. Kapetanovic, B. Ransford, and J. R. Smith, "WISPCam: A battery-free RFID camera," in *Proc. IEEE Int. Conf. RFID (RFID)*, 2015, pp. 166–173.

[20] A. Gomez, L. Sigrist, T. Schalch, L. Benini, and L. Thiele, "Efficient, long-term logging of rich data sensors using transient sensor nodes," *ACM Trans. Embedded Comput. Syst.*, vol. 17, no. 1, pp. 1–23, 2017.

[21] J. Hester and J. Sorber, "The future of sensing is batteryless, intermittent, and awesome," in *Proc. 15th ACM Conf. Embedded Netw. Sensor Syst. (Sensys)*, 2017, p. 21.

[22] B. Lucia, V. Balaji, A. Colin, K. Maeng, and E. Ruppel, "Intermittent computing: Challenges and opportunities," in *Proc. 2nd Summit Adv. Program. Lang. (SNAPL)*, 2017, pp. 1–14.

[23] J. Hester and J. Sorber, "Batteries not included," *ACM Mag. Students*, vol. 26, no. 1, pp. 23–27, 2019.

[24] S. Ahmed, N. A. Bhatti, M. H. Alizai, J. H. Siddiqui, and L. Mottola, "Efficient intermittent computing with differential checkpointing," in *Proc. 20th ACM SIGPLAN/SIGBED Int. Conf. Lang. Compilers Tools Embedded Syst.*, 2019, pp. 70–81.

[25] A. Colin, G. Harvey, B. Lucia, and A. P. Sample, "An energy-interference-free hardware-software debugger for intermittent energy-harvesting systems," *ACM SIGARCH Comput. Archit. News*, vol. 44, no. 2, pp. 577–589, 2016.

[26] A. Colin, E. Ruppel, and B. Lucia, "A reconfigurable energy storage architecture for energy-harvesting devices," in *Proc. 23rd Int. Conf. Architect. Support Program. Lang. Oper. Syst.*, 2018, pp. 767–781.

[27] N. Jackson, J. Adkins, and P. Dutta, "Capacity over capacitance for reliable energy harvesting sensors," in *Proc. 18th Int. Conf. Inf. Process. Sensor Netw.*, 2019, pp. 193–204.

[28] H.-X. Zou *et al.*, "Mechanical modulations for enhancing energy harvesting: Principles, methods and applications," *Appl. Energy*, vol. 255, Dec. 2019, Art. no. 113871.

[29] H. Jiang, M. E. Kiziroglou, D. C. Yates, and E. M. Yeatman, "A motion-powered piezoelectric pulse generator for wireless sensing via fm transmission," *IEEE Internet Things J.*, vol. 2, no. 1, pp. 5–13, Feb. 2015.

[30] S. Fang, X. Fu, X. Du, and W.-H. Liao, "A music-box-like extended rotational plucking energy harvester with multiple piezoelectric cantilevers," *Appl. Phys. Lett.*, vol. 114, no. 23, 2019, Art. no. 233902.

[31] G. Hu, L. Tang, J. Liang, and R. Das, "A tapered beam piezoelectric energy harvester shunted to P-SSHI interface," in *Proc. Active Passive Smart Struct. Integr. Syst. IX*, vol. 11376, 2020, p. 1137606.

[32] H. Fu and E. M. Yeatman, "Effective piezoelectric energy harvesting using beam plucking and a synchronized switch harvesting circuit," *Smart Mater. Struct.*, vol. 27, no. 8, 2018, Art. no. 084003.

[33] K. Fan, H. Qu, Y. Wu, T. Wen, and F. Wang, "Design and development of a rotational energy harvester for ultralow frequency vibrations and irregular human motions," *Renew. Energy*, vol. 156, pp. 1028–1039, Aug. 2020.

[34] F. Li, Y. Yang, Z. Chi, L. Zhao, Y. Yang, and J. Luo, "Trinity: Enabling self-sustaining WSNs indoors with energy-free sensing and networking," *ACM Trans. Embedded Comput. Syst.*, vol. 17, no. 2, pp. 1–27, 2018.

[35] Q. Huang, Y. Mei, W. Wang, and Q. Zhang, "Toward battery-free wearable devices: The synergy between two feet," *ACM Trans. Cyber Phys. Syst.*, vol. 2, no. 3, pp. 1–18, 2018.

[36] Y. Kuang, T. Ruan, Z. J. Chew, and M. Zhu, "Energy harvesting during human walking to power a wireless sensor node," *Sensors Actuators A Phys.*, vol. 254, pp. 69–77, Feb. 2017.

[37] Y. Huang *et al.*, "Preliminary testing of a hand gesture recognition wristband based on EMG and inertial sensor fusion," in *Proc. Int. Conf. Intell. Robot. Appl.*, 2015, pp. 359–367.

[38] S. Jiang, B. Lv, X. Sheng, C. Zhang, H. Wang, and P. B. Shull, "Development of a real-time hand gesture recognition wristband based on SEMG and IMU sensing," in *Proc. IEEE Int. Conf. Robot. Biomimet. (ROBIO)*, 2016, pp. 1256–1261.

[39] O. D. Lara and M. A. Labrador, "A survey on human activity recognition using wearable sensors," *IEEE Commun. Surveys Tuts.*, vol. 15, no. 3, pp. 1192–1209, 3rd Quart., 2012.

[40] A. J. Bandodkar *et al.*, "Battery-free, skin-interfaced microfluidic/electronic systems for simultaneous electrochemical, colorimetric, and volumetric analysis of sweat," *Sci. Adv.*, vol. 5, no. 1, 2019, Art. no. eaav3294.

[41] G. Valdés-Ramírez *et al.*, "Microneedle-based self-powered glucose sensor," *Electrochem. Commun.*, vol. 47, pp. 58–62, Oct. 2014.

[42] Z. Wang, V. Leonov, P. Fiorini, and C. Van Hoof, "Realization of a wearable miniaturized thermoelectric generator for human body applications," *Sensors Actuators A Phys.*, vol. 156, no. 1, pp. 95–102, 2009.

[43] V. Leonov, T. Torfs, R. J. Vullers, J. Su, and C. Van Hoof, "Renewable energy microsystems integrated in maintenance-free wearable and textile-based devices: The capabilities and challenges," in *Proc. IEEE Int. Conf. Ind. Technol.*, 2010, pp. 967–972.

[44] V. Leonov, T. Torfs, P. Fiorini, and C. Van Hoof, "Thermoelectric converters of human warmth for self-powered wireless sensor nodes," *IEEE Sensors J.*, vol. 7, no. 5, pp. 650–657, May 2007.

[45] V. Leonov and R. Vullers, "Wearable thermoelectric generators for body-powered devices," *J. Electron. Mater.*, vol. 38, no. 7, pp. 1491–1498, 2009.

[46] X. Wang, "Intelligent multi-camera video surveillance: A review," *Pattern Recognit. Lett.*, vol. 34, no. 1, pp. 3–19, 2013.

[47] F. Adib, Z. Kabelac, D. Katabi, and R. C. Miller, "3D tracking via body radio reflections," in *Proc. 11th USENIX Symp. Netw. Syst. Design Implement. (NSDI)*, 2014, pp. 317–329.

[48] J. Mi, L. Xu, Z. Zhu, M. Liu, and L. Zuo, "Design, modeling and testing of a one-way energy harvesting backpack," in *Proc. Active Passive Smart Struct. Integr. Syst. XII*, vol. 10595, 2018, Art. no. 1059520.

[49] W. McArdle, F. Katch, and V. Katch, *Exercise Physiology: Nutrition, Energy, and Human Performance*, 7th ed. Vancouver, BC, Canada: Langara College, 2009.

[50] D. A. Winter, *Biomechanics and Motor Control of Human Movement*. Hoboken, NJ, USA: Wiley, 2009.

[51] M. Cai, Z. Yang, J. Cao, and W.-H. Liao, "Recent advances in human motion excited energy harvesting systems for wearables," *Energy Technol.*, vol. 8, no. 10, 2020, Art. no. 2000533.

[52] H. Liu, J. Zhong, C. Lee, S.-W. Lee, and L. Lin, "A comprehensive review on piezoelectric energy harvesting technology: Materials, mechanisms, and applications," *Appl. Phys. Rev.*, vol. 5, no. 4, 2018, Art. no. 041306.

[53] P. Pillatsch, E. M. Yeatman, and A. S. Holmes, "A piezoelectric frequency up-converting energy harvester with rotating proof mass for human body applications," *Sensors Actuators A Phys.*, vol. 206, pp. 178–185, Feb. 2014.

[54] P. Pillatsch, E. Yeatman, and A. Holmes, "Magnetic plucking of piezoelectric beams for frequency up-converting energy harvesters," *Smart Mater. Struct.*, vol. 23, no. 2, 2013, Art. no. 025009.

[55] M. Pozzi and M. Zhu, "Plucked piezoelectric bimorphs for knee-joint energy harvesting: Modelling and experimental validation," *Smart Mater. Struct.*, vol. 20, no. 5, 2011, Art. no. 055007.

[56] M. Pozzi, M. S. Aung, M. Zhu, R. K. Jones, and J. Y. Goulermas, "The pizzicato knee-joint energy harvester: Characterization with biomechanical data and the effect of backpack load," *Smart Mater. Struct.*, vol. 21, no. 7, 2012, Art. no. 075023.

[57] Y. Kuang and M. Zhu, "Design study of a mechanically plucked piezoelectric energy harvester using validated finite element modelling," *Sensors Actuators A Phys.*, vol. 263, pp. 510–520, Aug. 2017.

[58] A. Wickenheiser and E. Garcia, "Broadband vibration-based energy harvesting improvement through frequency up-conversion by magnetic excitation," *Smart Mater. Struct.*, vol. 19, no. 6, 2010, Art. no. 065020.

[59] W. Al-Ashtari, M. Hunstig, T. Hemsel, and W. Sextro, "Frequency tuning of piezoelectric energy harvesters by magnetic force," *Smart Mater. Struct.*, vol. 21, no. 3, 2012, Art. no. 035019.

[60] H. Fu and E. M. Yeatman, "Rotational energy harvesting using bi-stability and frequency up-conversion for low-power sensing applications: Theoretical modelling and experimental validation," *Mech. Syst. Signal Process.*, vol. 125, pp. 229–244, Jun. 2019.

[61] X. Li *et al.*, "ViPSN: A vibration-powered IoT platform," *IEEE Internet Things J.*, vol. 8, no. 3, pp. 1728–1739, Feb. 2021.

[62] J. Liang and W.-H. Liao, "Improved design and analysis of self-powered synchronized switch interface circuit for piezoelectric energy harvesting systems," *IEEE Trans. Ind. Electron.*, vol. 59, no. 4, pp. 1950–1960, Apr. 2012.

[63] M. Ferrari, V. Ferrari, M. Guizzetti, B. Ando, S. Baglio, and C. Trigona, "Improved energy harvesting from wideband vibrations by nonlinear piezoelectric converters," *Sensors Actuators A Phys.*, vol. 162, no. 2, pp. 425–431, 2010.

[64] S. Balakrishnan, V. Sundaresan, V. Krishnan, and S. R. Aravindababu, "Nonlinear dynamics of asymmetric bistable energy harvesting systems," in *Proc. AIP Conf.*, vol. 2134, 2019, Art. no. 080004.

[65] K. Zhao, Y. Zhao, and J. Liang, "A vibration-powered Bluetooth wireless sensor node with running PFC power conditioning," in *Proc. IEEE Int. Symp. Circuits Syst. (ISCAS)*, 2017, pp. 1–4.
[66] *LTC3588-1 Data Sheet*, Linear Technol., Milpitas, CA, USA.
[67] *MIC841/2 Data Sheet*, Microchip Technol., Chandler, AZ, USA.
[68] *nRF52832 Data Sheet*, Nordic Semicond., Trondheim, Norway.

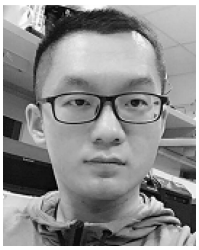

Xin Li (Graduate Student Member, IEEE) received the B.E. and B.Ec. degrees from the North University of China, Taiyuan, China, in 2016. He is currently pursuing the Ph.D. degree with the School of Information Science and Technology, ShanghaiTech University, Shanghai, China.

He is also with the Shanghai Institute of Microsystem and Information Technology, Chinese Academy of Sciences, Beijing, China, and with the University of Chinese Academy of Sciences, Beijing. His research interests include kinetic/vibration energy harvesting, intermittent computing, ubiquitous computing, and Internet of Things.

Dr. Li was a recipient of the First Place of the International Conference on Embedded Wireless Systems and Networks Dependability Competition in 2019 and the First Runner Up of the IEEE Industrial Electronics Society Inter-Chapter Paper Competition in 2019.

Hong Tang received the B.E. degree in telecommunication engineering from Fuzhou University, Fuzhou, China, in 2017. He is currently pursuing the master's degree with the School of Information Science and Technology, ShanghaiTech University, Shanghai, China.

His research interests includes vibration-powered IoT system and mobile computing, especially their power solution, cyber-electromechanical synergy, and applications of IoT systems.

Guobiao Hu received the B.E. degree from Southwest Jiaotong University, Chengdu, China, in 2012, the Diplôme d'Ingénieur from École Centrale Paris, Châtenay-Malabry, France, in 2015, and the Ph.D. degree from the University of Auckland, Auckland, New Zealand, in 2020.

In 2020, he was a Postdoctoral Research Fellow with the School of Information Science and Technology, ShanghaiTech University, Shanghai, China. He is currently a Postdoctoral Research Fellow with the School of Civil and Environmental Engineering, Nanyang Technological University, Singapore. His research interests include vibration/wind energy harvesting and acoustic-elastic metamaterials.

Dr. Hu is a recipient of the Best Paper Finalist Award in the SPIE conference on Smart Structures/NDE in 2018.

Bao Zhao (Graduate Student Member, IEEE) received the B.E. degree from Harbin Engineering University, Harbin, China, in 2017, and the M.E. degree from a joint program of ShanghaiTech University, Shanghai, China, and University of Chinese Academy of Sciences, Beijing, China, in 2020.

His current research interests include energy harvesting, power electronics, and mechatronics.

Junrui Liang (Senior Member, IEEE) received the B.E. and M.E. degrees in instrumentation engineering from Shanghai Jiao Tong University, Shanghai, China, in 2004 and 2007, respectively, and the Ph.D. degree in mechanical and automation engineering from Chinese University Hong Kong, Hong Kong, in 2010.

He is currently an Assistant Professor with the School of Information Science and Technology, ShanghaiTech University, Shanghai. His research interests include: energy conversion and power conditioning circuits, kinetic energy harvesting and vibration suppression, IoT devices, and mechatronics.

Dr. Liang is a recipient of two Best Paper Awards in the IEEE International Conference on Information and Automation (2009 and 2010, respectively). He is an Associate Editor of *IET Circuits, Devices and Systems* and the General Chair of the 2nd International Conference on Vibration and Energy Harvesting Applications 2019.